A hydrodynamic simulation on reactive shock attenuation in the large-scale gap test of heavily aluminized RDX

Bohoon Kim, Minsung Kim and Jack J. Yoh*
Department of Mechanical and Aerospace Engineering, Seoul National University
Seoul, Korea 151-742

1 Introduction

Pyrotechnic initiators having a gap or a through bulkhead material between donor and acceptor are used to ignite more difficult-to-ignite energetic materials. The operability of initiator depends on the shock sensitivity of gap and high explosive combination. A gap test is a standardized test to quantify shock sensitivity of an acceptor that one tries to characterize. The critical thickness of a gap whose shock characteristics are known a priori is measured as the acceptor charge is detonated at a corresponding pressure [1,2].

The gap test has one great advantage over other commonly used method for measuring the sensitivity such as drop-weight impact test [3]. It has been reported that the critical gap thickness, under highly controlled circumstances, is quite reproducible with the error less than a fraction of a millimeter [4].

The components for the test consists of four parts: donor charge, attenuating gap, acceptor charge and a witness block. The four components are arranged in series as such a donor is detonated first by an electrical means. The shock wave generated by the detonation reaches the gap and its strength attenuates while passing through the gap of a specified thickness. The transmitted shock wave then may or may not trigger the acceptor charge depending on the level of attenuation of the triggering shock wave. If detonated, a hole is created at the witness block. Otherwise, the block suffers a minor geometric deformation. Here, gap thickness is adjusted and the test is repeated until a critical thickness (go/nogo) is witnessed for the test sample (acceptor charge). A critical gap thickness for which the acceptor has 50% probability of being detonated, provides the quantification of shock sensitivity of the acceptor charge [5,6].

In this paper, we attempt to defining a clear multi-material analysis for a standardized large-scale gap test (LSGT) that is comprised of donor (Pentolite), gap (PMMA), and an acceptor (heavily aluminized RDX). The full scale numerical simulation is performed which provides the quantitative sensitivity response of the system. The donor charge is comprised of 50% RDX (cyclotrimethylene-trinitramine, $C_3H_6N_6O_6$), 35% aluminum powder, and 15% HTPB (hydroxyl-terminated polybutadiene) binder. Its initial density after pressing is 1.78 g/cc. The results provide the complex shock interaction structure, the critical gap thickness, and the corresponding detonation characteristics within the acceptor charge following the complex interaction with PMMA gap. All the results are compared against the experimental measurements, which are used in the initial designing of a new pyrotechnic initiator.

2 Approach

Correspondence to: jjyoh@snu.ac.kr

In order to simulate the energetic response of high explosive system accompanied by high temperature and pressure conditions, one requires a reactive flow model, casing rupture model, multi-material interface tracking model and eigenvalue capturing model. Eigenvalue capturing model tracks the propagation of the signal speeds at u, $u+c$ and $u-c$ where u and c are particle velocity and sound speed, respectively. For both fluids and solids, compressible conservation equations are used, and the stresses within the solid is composed of deviatoric stress and hydrostatic pressure [7]. The Mie-Gruneisen form EOS (Equation of State) is used for pressure of solid, while the JWL (Jones-Wilkins-Lee) EOS is used for the explosive. The rate of chemical reaction is based on the Ignition and Growth frame work previously built for the heavily aluminized RDX [8]. The interface between two different materials is tracked through a hybrid particle level set method, and the material properties near the interface are determined through the ghost fluid method.

Compressible Navier-Stokes Equation

The governing equations in a cylindrical coordinate system reflect the conservation laws of mass, momentum, and energy.

$$\frac{\partial \vec{U}}{\partial t} + \frac{\partial \vec{E}}{\partial r} + \frac{\partial \vec{F}}{\partial z} = \vec{S}\left(\vec{U}\right) \tag{1}$$

$$\vec{U} = \begin{bmatrix} \rho \\ \rho u_r \\ \rho u_z \\ \rho E \end{bmatrix}, \quad \vec{E} = \begin{bmatrix} \rho u_r \\ \rho u_r^2 + p \\ \rho u_r u_z \\ u_r(\rho E + p) \end{bmatrix}, \quad \vec{F} = \begin{bmatrix} \rho u_z \\ \rho u_z u_r \\ \rho u_z^2 + p \\ u_z(\rho E + p) \end{bmatrix}, \tag{2}$$

$$\vec{S} = \begin{bmatrix} -\dfrac{\rho u_r}{r}\varphi \\ \dfrac{s_{rr} - s_{\theta\theta} - \rho u_r^2}{r}\varphi + \eta\left(\dfrac{\partial s_{rr}}{\partial r} + \dfrac{\partial s_{zr}}{\partial z}\right) \\ \dfrac{s_{zr} - \rho u_r u_z}{r}\varphi + \eta\left(\dfrac{\partial s_{rz}}{\partial r} + \dfrac{\partial s_{zz}}{\partial z}\right) \\ \dfrac{u_r s_{rr} + u_z s_{rz} - u_r(\rho E + p)}{r}\varphi + \eta\left(\dfrac{\partial (u_r s_{rr} + u_z s_{rz})}{\partial r} + \dfrac{\partial (u_r s_{zr} + u_z s_{zz})}{\partial z}\right) \end{bmatrix} \tag{3}$$

where φ = 0, 1 for rectangular and cylindrical coordinates respectively and η = 0, 1 for fluids (liquids and gases) and solids respectively. The governing equation is solved by third-order Runge-Kutta and ENO (essentially non-oscillatory) method with respect to the temporal and spatial discretization respectively.

Here, the stress state of the solid state unreacted explosives is ignored due to its insignificant contribution during the explosive pressure rise upon initiation. However, the stress state of the inert confinement is considered by separating the Cauchy stress into deviatoric and hydrostatic tensors following the isotropic postulation.

$$\sigma_{ij} = s_{ij} - p\delta_{ij} \tag{4}$$

The deviatoric stress changes with respect to time as the following differential equation.

$$\overset{\&}{s}_{ij} = \overset{\&}{s}_{ij,tr} + \overset{\&}{s}_{ij,cor} = \Omega_{ik}s_{kj} - s_{ik}\Omega_{kj} + 2G(\overline{D_{ij}} - D_{ij}^{p}) \tag{5}$$

$$\overset{\&}{s}_{ij,tr} = \Omega_{ik}s_{kj} - s_{ik}\Omega_{kj} + 2G\overline{D_{ij}} \tag{6}$$

$$\overset{\&}{s}_{ij,cor} = -H : D_{ij}^{p} = -2G\Lambda N_{ij,tr} \tag{7}$$

where.

$$\overline{D}_{ij} = D_{ij} - \frac{1}{3} D_{kk}\delta_{ij}, \quad D_{ij} = \frac{1}{2}\left(\frac{\partial u_i}{\partial x_j} + \frac{\partial u_j}{\partial x_i}\right), \quad \Omega_{ij} = \frac{1}{2}\left(\frac{\partial u_i}{\partial x_j} - \frac{\partial u_j}{\partial x_i}\right) \tag{8}$$

Constitutive Relation

The JWL form equations for acceptor and shock Hugoniot for donor were used as the EOS of the unreacted high explosives as follows.

$$p_{unreacted\,(\text{acceptor})} = Ae^{-R_1(\rho_0/\rho)} + Be^{-R_2(\rho_0/\rho)} + \omega e_0\left(\rho_0/\rho\right)^{-1} \tag{9}$$

$$p_{unreacted\,(\text{donor})} = A\left(\rho/\rho_0 - 1\right)^1 + B\left(\rho/\rho_0 - 1\right)^2 + C\left(\rho/\rho_0 - 1\right)^3 \tag{10}$$

Especially an isentropic JWL C-term form is used for products, and is derived assuming the process is isentropic.

$$p_{reacted\,(\text{donor, acceptor})} = Ae^{-R_1(\rho_0/\rho)} + Be^{-R_2(\rho_0/\rho)} + C\left(\rho_0/\rho\right)^{-(1+\omega)} \tag{11}$$

As for the solid gap material, Mie-Gruneisen form EOS is adapted to calculate the pressure within.

$$p(\rho, e) = \rho_0\Gamma_0 e + \begin{cases} \dfrac{\rho_0 c_0^2\varphi}{(1-s\varphi)^2}\left[1 - \dfrac{\Gamma_0}{2}\varphi\right] & if\ \rho \geq \rho_0 \\ c_0^2(\rho - \rho_0) & otherwise \end{cases} \tag{12}$$

where $\varphi = 1-\rho_0/\rho$. The Johnson–Cook model is used to determine the critical stress before plastic deformation. This model makes use of equivalent plastic strain, strain rate and melting temperature. The form of the equation is as follows.

$$\sigma_Y = \left(A + B(\overline{\varepsilon^p})^n\right)\left(1 + C\ln(\frac{\dot{\overline{\varepsilon^p}}}{\dot{\varepsilon}_n})\right)\left(1 - \frac{T - T_0}{T_m - T_0}\right) \tag{13}$$

Since the gap of PMMA is brittle enough and thus no such strength model is required, a constant yield works well in the present work. The yield stress of PMMA is a fixed value, and it becomes zero if temperature exceeds the melting temperature.

Chemical Reaction of the High Explosive Material

The reactive flow model uses the rate of product mass fraction consisting of ignition and growth suggested by Kim *et al*. [8].

$$\frac{d\lambda}{dt} = I(1-\lambda)\mu^a + G(1-\lambda)p^b, \ \mu = \frac{\rho}{\rho_0} - 1 \tag{14}$$

Here p is the pressure, t is time, ρ_0 and ρ are the initial and current densities, respectively. λ is the burned mass fraction, and constants I, a, G, b are the determined parameters. λ is reaction progress variable ($\lambda = 0$ unreacted state and $\lambda = 1$ reacted state) and the compression term, μ, is defined as ($\mu = \rho/\rho_0$-1). The rate law is comprised of *i*) ignition term that represents formation of the hotspots by the rapid compression, and *ii*) growth term that describes the effect of the propagation of the reacting waves in the substance. Four unknown parameters having the major significance in view of detonation are determined based on a series of rate stick experiments and previously validated for the present explosive materials [8].

3 Gap Test and Simulation

To simulate Pentolite-PMMA-aluminized RDX configuration of the LSGT, we adopt the modeling constants from the various references. Table 1 summarizes material properties of PMMA and its Mie-Gruneisen EOS. Table 2 lists the chemical reaction and growth parameters of donor (pentolite) and acceptor (aluminized RDX). In particular, the donor is a well-known explosive whose JWL EOS parameters are obtained by the CHEETAH calculation.

Table 1. Modeling constants for PMMA

Mechanical constant		*Mie-Gruneisen EOS*	
Initial density (kg/m^3)	1182	C_0 (m/s)	2180
Young's modulus (GPa)	0.42	S_0	1.410
Shear modulus (GPa)	2.32	Gruneisen coefficient	0.85
Thermal constant		*Strength model*	
Specific heat capacity(J/kg·K)	1466	Constant yield stress (GPa)	0.42
Room temperature (K)	300		
Melt temperature (K)	330.3		

Table 2. Modeling constants for heavily aluminized RDX

	Model parameter	Pentolite	Aluminized RDX
Reactant	ρ_0 (kg/m^3)	1560	1780
	A (GPa)	12.82	15270
	B (GPa)	0	-5.175
	e_0 (GPa)	-	0.706
	C (GPa)	119.3	-
	R_1	-	9.500
	R_2	-	0.950
	w (J/g-K)	-	0.976
Product	A (GPa)	507.91	2633.31
	B (GPa)	6.620	8.590
	C (GPa)	1.270	1.090
	R_1	4.620	6.680
	R_2	1.020	1.110
	w (J/g-K)	0.330	0.090
Chemical kinetics	I (s^{-1})	1.4x10^8	3.2x10^8
	A	4.0	4.0
	G (s^{-1} Mbar^{-b})	3.3x10^8	3.5x10^7
	B	1.3	0.7
	p_i (GPa)	-	5.9

Gap test was conducted to estimate the sensitivity of the target acceptor charge, namely a heavily aluminized RDX. The setup is quite simple and judgment on Go/NoGo is unambiguous. The gap test configuration is illustrated in Fig. 1. The donor charge is a Pentolite of which initial density is 1.56 g/cc, and the acceptor is an aluminized RDX of which initial density is 1.78 g/cc. The gap is provided by stacking PMMA discs to adjust the its thickness height. All materials were shaped into a 50.8 mm diameter circle. The height of donor is 50.8 mm and that of acceptor is 139.7 mm. Three trials are conducted at gap thicknesses varied by 0.254 mm interval. Go/NoGo criterion is obtained until the witness plate breakage. In the experimental test, the critical thickness was 25.75 mm as any other gap thickness below this value, witness plate was virtually undamaged.

The schematic of the gap test simulation is shown in Fig. 2. The gap sizes are varied from 15 mm to 30 mm with 1 mm interval. As for the initial condition for starting donor detonation, 1 km/s impact is used at the bottom of the donor. All other outer boundaries are unconfined. Shown in Fig. 3 are the reaction progress variable (λ) and pressure for both donor and acceptor while density is used for PMMA. Two cases are compared where 25 mm gap thickness result (a) and 26 mm case is shown in (b). Clearly seen, the detonation failure is noted at 26 mm case where the attenuated shock wave fails to detonate the acceptor charge of aluminized RDX. It must that the critical thickness lies between 25 and 26 mm, as is consistent with the experimental observation.

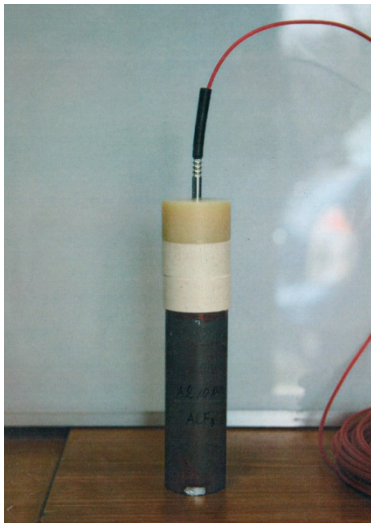

Figure 1. Gap test configurations.

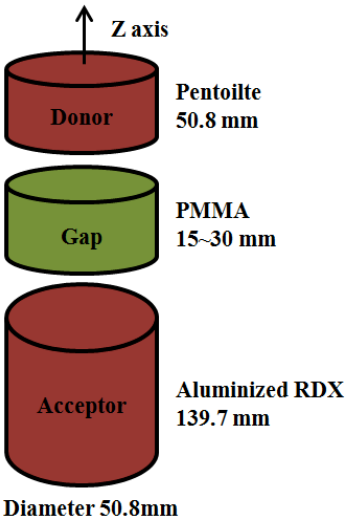

Figure 2. Schematic of gap simulation.

Table 3. LSGT test result

PMMA gap thickness	Go/No go
24.480mm	Go
24.734mm	Go
24.988mm	Go
25.242mm	Go
25.496mm	Go
25.750mm	Go/NoGo
26.004mm	No go
26.258mm	No go
26.512mm	No go
26.766mm	No go
27.020mm	No go

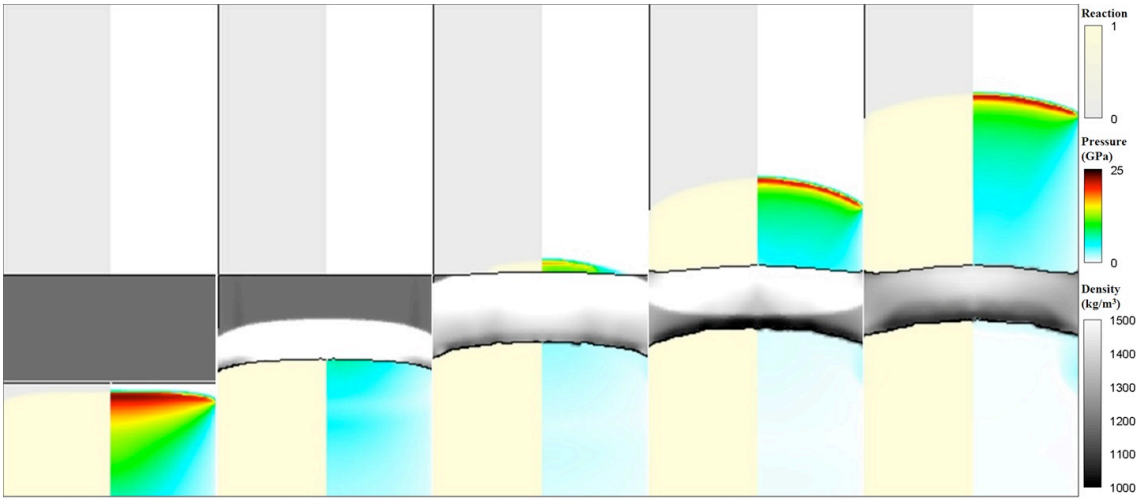

(a) Go Case at 25 mm PMMA thickness

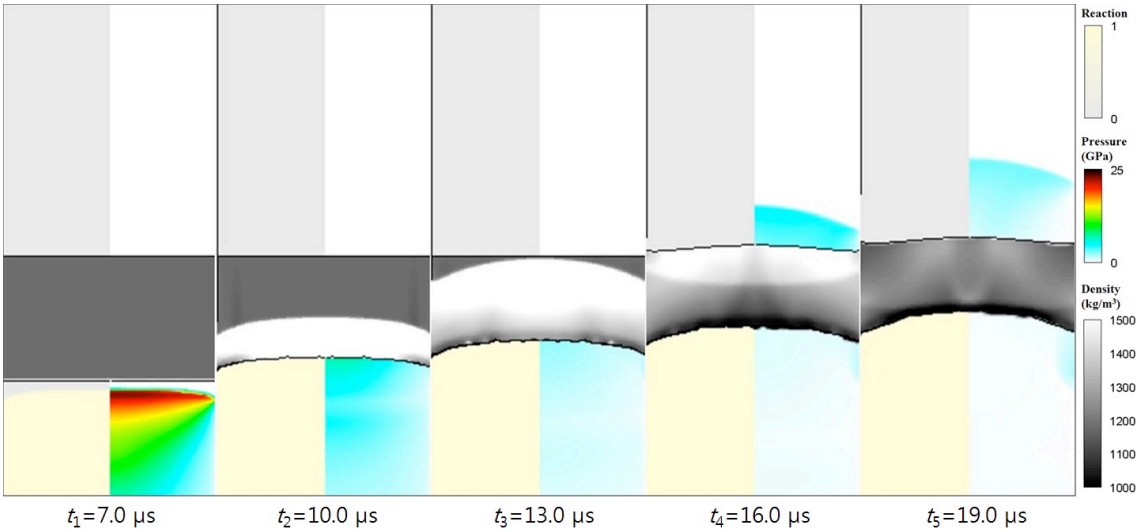

(b) Nogo Case at 26 mm PMMA thickness

Figure 3. Shown reaction progress and pressure for donor/acceptor, density for PMMA. 25 mm Gap (a) and 26 mm Gap (b)

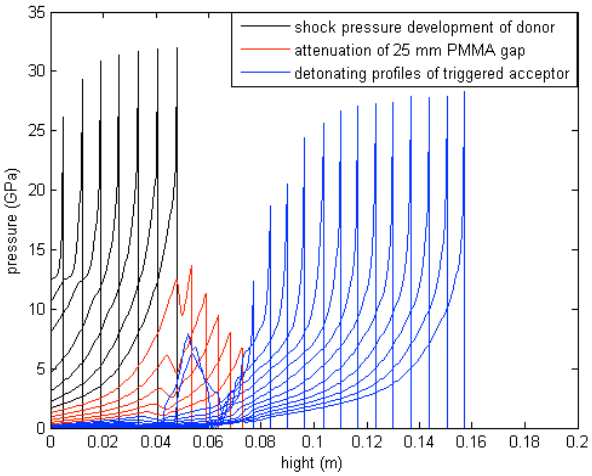

Figure 4. Time trace of consecutive pressure profiles of LSGT simulation with 25 mm PMMA gap

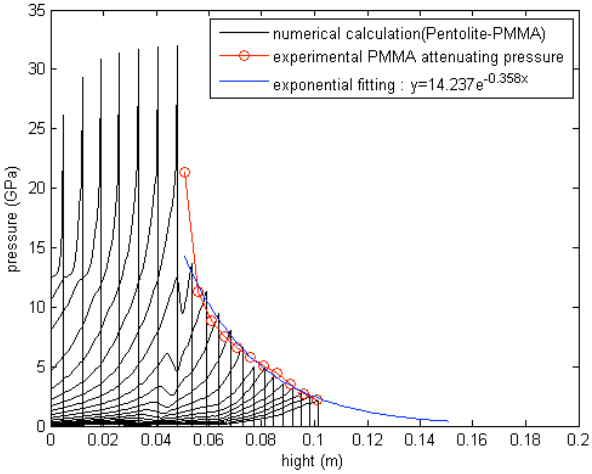

Figure 5. Comparison of attenuating pressure distributions along the gap thickness.

The time trace of consecutive pressure profiles along the centerline of LSGT simulation with 25 mm PMMA gap which is a Go case is shown in Fig. 4. In the beginning of the test, the shock pressure is developed along the Pentolite donor up to 32 GPa. The shock strength is reduced as it passes through the attenuating gap. After mitigated to a certain degree, the shock triggers the acceptor charge. At this moment, the critical initiating pressure was 5.9 GPa.
Figure 5 shows the comparison of attenuating pressure distribution along the gap thickness. The result clearly demonstrates the reliable prediction of the shock sensitivity to the present LSGT.

Acknowledgment

Authors would like to thank the financial supports from Agency for Defense Development (HH-5) and Hanwha Corp. (PMD) contracted through the Institute of Advanced Aerospace Technology at Seoul National University.

References

[1] Muraour H. (1933) Note Sur la Determination de la Sensibilite au Choc des Explosifs. Mem. d'Artill. Fr., 12: 559.

[2] Liddiard TP, Jacobs SJ. (1965). The initiation of reactions in explosives by shocks. NOLTR 64-53.

[3] Storm CB et al. (1990). Sensitivity relationships in energetic materials. Chem. and Phys. of Energ. Mat. 605.

[4] Macek A. (1962). Sensitivity of explosives. Chem. Rev. 62: 41.

[5] Keshavarz MH et al. (2007). Prediction of shock sensitivity of explosives based on small-scale gap test. J. Haz. Mat. 145: 109.

[6] Kubota et al. (2006). Observation of shock initiation process in gap test. AIP Conf. Proc. 845: 1085.

[7] Kim K, Yoh JJ. (2013). A particle level-set based Eulerian method for multi-material detonation simulation of high explosive and metal confinements. Proc. of the Comb. Inst. 34: 2025.

[8] Kim B et al. (2014). A reactive flow model for heavily aluminized cyclotrimethylene-trinitramine. J. App. Phy. 116: 023512.